The Use of Peak Functions in Heat Load Modeling of District Heating System

Erik Král, Lubomír Vašek. Viliam Dolinay, Petr Čápek

***Abstract*—**This paper describes the use of peak functions in the heat load modeling of district heating system. Heat load is approximated by the sum of time dependent and temperature dependent components. The temperature dependent component is approximated using sum of two peak functions and temperature dependent component is approximated using generalized logistic function. The model parameters are estimated using Particle Swarm Algorithm.

***Keywords*—**District Heating, Heat load, Modeling, Peak function, Particle swarm, Approximation.

I. Introduction

This paper describes the usage of peak functions in heat load modeling of heat distribution and consumption in municipal heating network. Heat load is approximated by the sum of time dependent and temperature dependent components. There are several approaches for heat load modeling [1]-[7]. We have proposed new approximation based method, where the temperature dependent component is approximated using sum of two peak functions. We use the Hybrid of Gaussian and truncated exponential functions (EGH) [6].

The temperature dependent component is approximated using generalized logistic function. The model parameters are estimated using Particle Swarm Optimization (PSO) Algorithm [10]. Method was implemented as algorithm in JAVA language and was evaluated on the data of two combined heat and power plants (CHP). This paper presents calculation of delivered heat load, approximation model, PSO variant, stopping criterion and related cost function. Finally, the experiment results are presented.

II. Heat Load Estimation

A. Primary and Secondary Side

A district heating system consists of primary side (heat producer) and secondary side (heat consumer) (Fig. 1). We are modeling heat load supplied to the district heating system.

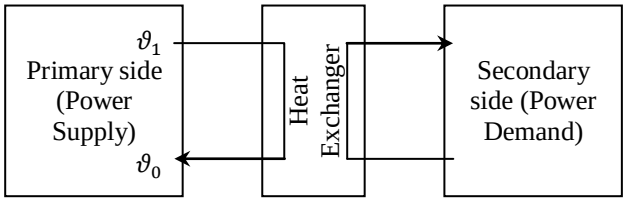

Fig. 1: Primary and Secondary side

where

ϑ_1	$°C$	is supply temperature,
ϑ_0	$°C$	is return temperature.

B. Transport Times

Transport time of the supply line can be calculated according to [8]:

$$R = \int_{t-T_{D1}}^{t} \dot{m}(\tau)\, d\tau \tag{1}$$

where

R	kg	is the known mass volume,
T_{D1}	s	is the unknown supply line transport time,
$\dot{m}(t)$	$\frac{kg}{s}$	is the measured mass flow at time τ.

Algorithm for estimation transport time of supply line is depicted in Fig. 2. The mass volume R is measured from known parameters of distribution network or is set by optimization algorithm.

Transport time of the return line can be calculated according to [8] and this process is depicted in Fig. 3:

$$R = \int_{t}^{t+T_{D0}} \dot{m}(\tau)\, d\tau \tag{2}$$

where

T_{D0}	is the unknown transport time of return line.

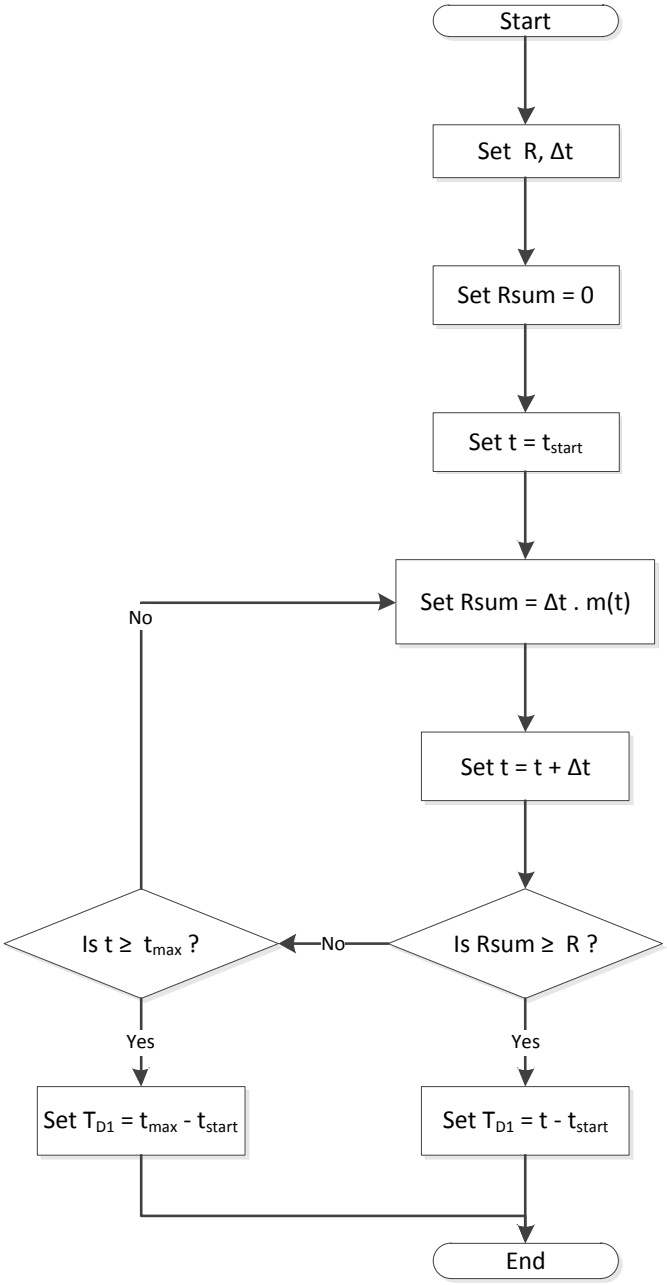

Fig. 2: Calculation of transport time of the supply line

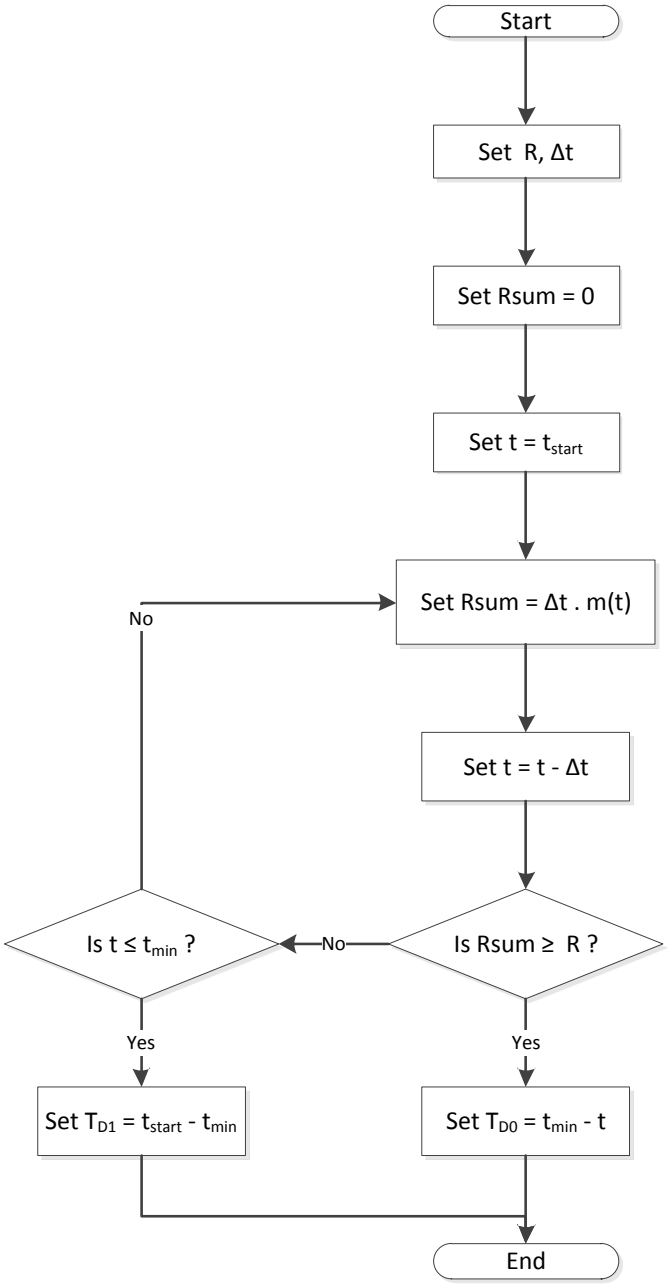

Fig. 3: Calculation of transport time of the return line

C. Delivered Heat Load

District heating system is approximated by load centre of mass of the system [8]:

$$P(t) = \dot{m}(t)c\left(\vartheta_1\left(t - \frac{T_{D1}}{2}\right) - \vartheta_0\left(t + \frac{T_{D0}}{2}\right)\right) \quad (3)$$

where

$P(t)$	W	is the heat load,
c	$\frac{J}{kg\,K}$	is the specific heat capacity,

Fig. 4 depicted delivered Heat Load to the CHP.

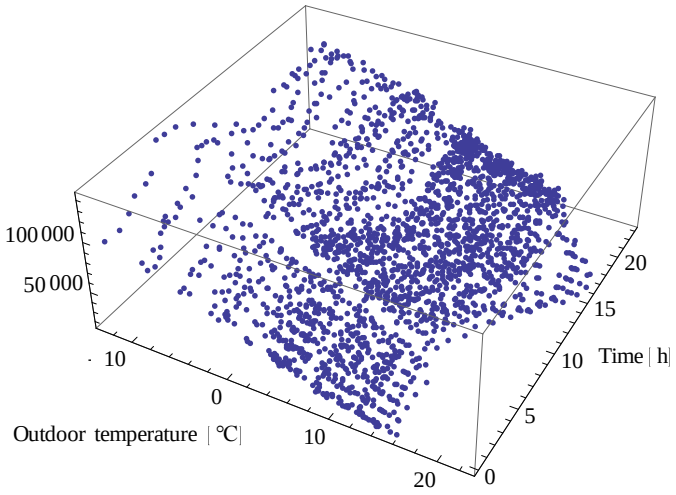

Fig. 4: Measuered Heat Load

III. Heat load approximation a prediction

Heat load is approximated by the sum of time dependent and temperature dependent components.

$$f_P(t, \vartheta_{ex}) = f_{time}(t) + f_{temp}(\vartheta_{ex}) \quad (4)$$

where

$f_{time}(t)$		is the time dependent, component,
t_0		is the time offset,
ϑ_{ex}	$°C$	is the outdoor temperature,
$f_{temp}(\vartheta_{ex})$		is the outdoor temperature, dependent component.

Fig. 5 shows approximation function.

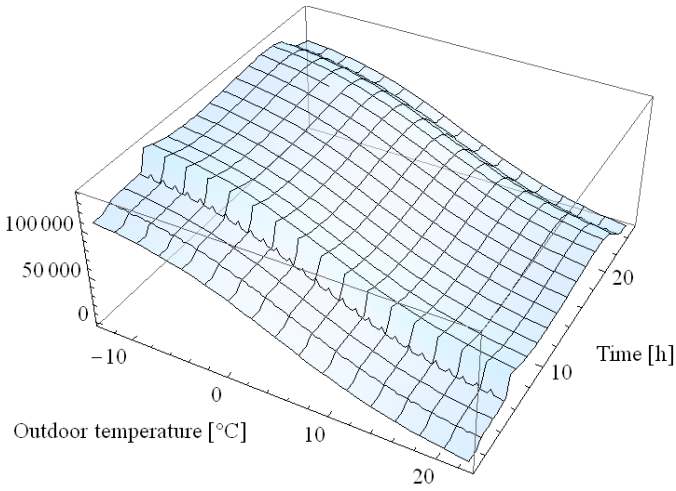

Fig. 5: Approximated heat load

A. Temperature Dependent Component

Temperature dependent component is approximated using generalized logistic function (Fig. 6).

$$f_{temp}(\vartheta_{ex}) = A + \frac{K - A}{(1 + Qe^{-B(\vartheta_{ex} - M)})^{\frac{1}{v}}} \quad (5)$$

where

A	is the lower asymptote,
K	is the upper asymptote,
Q	is the depend on the value $f_{temp}(0)$,
B	is the growth rate,
v	affects near which asymptote maximum growth occurs,
M	is the time of maximum growth if Q = v.

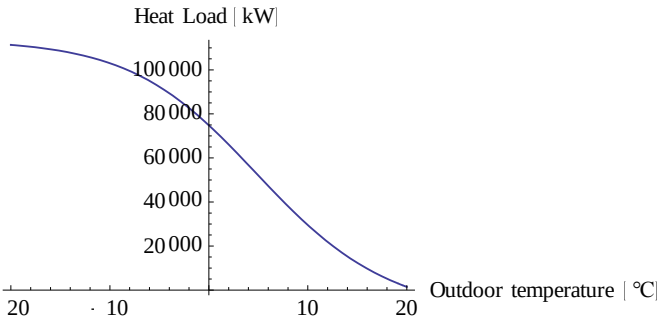

Fig. 6: Generalized logistic function

B. Time Dependent Component

The time dependent component is approximated by the sum of two peak functions. The Hybrid of Gaussian and truncated exponential function (EGH) [9] was selected as most the convenient function.

Hybrid of Gaussian and truncated exponential function is defined as

$$d = 2\sigma^2 + \tau(t - t_m)$$

$$f_{EGH}(t) = \begin{cases} H\, exp\left(\dfrac{-(t-t_m)^2}{d}\right), & d > 0 \\ 0, & d \le 0 \end{cases} \quad (6)$$

where

H	is the peak height,,
σ	is the standard deviation of the parent Gaussian peak,
τ	is the time constant of the precursor exponential decay,
k_L	is the parameter of the speed of the fall of the leading trail,
t_m	is the time of the peak.

$f_{time}(t)$ is the sum of two EGH functions:

$$f_{time}(t) = f_{EGH1}(t) + f_{EGH2}(t) \quad (7)$$

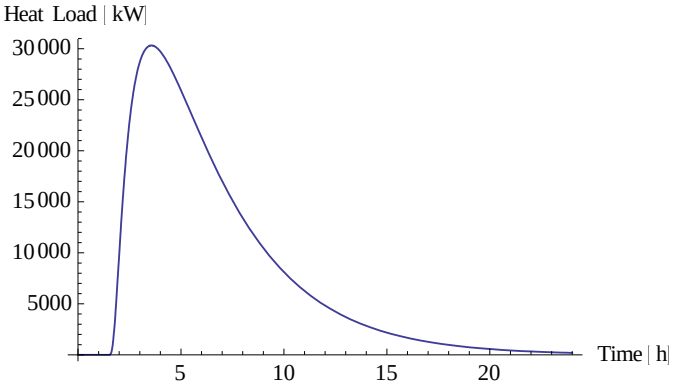

Fig. 7: Example of f_{EGH1} function

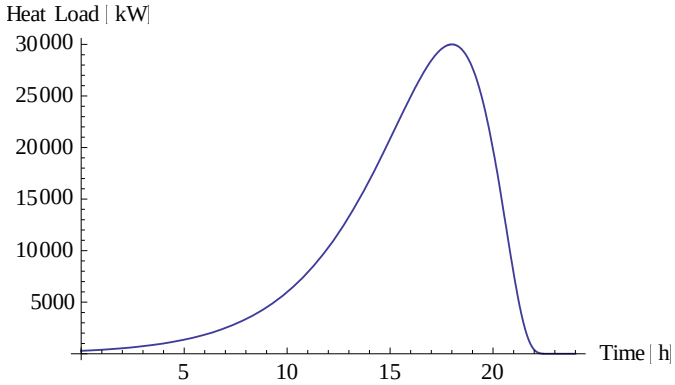

Fig. 8: Example of f_{EGH2} function

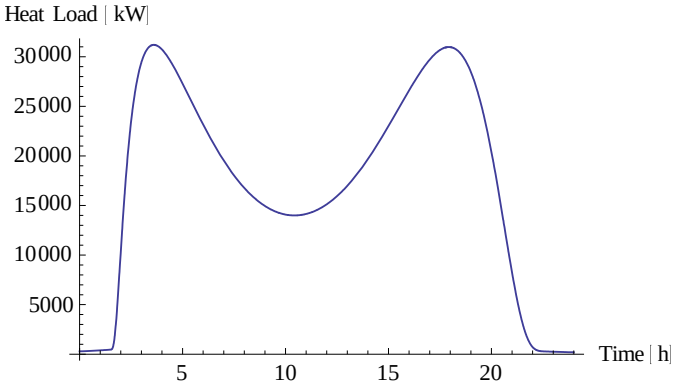

Fig. 9: Example of f_{time} function

C. Cost Function

Cost function using EGH functions is defined as

$$\min_{\beta} \sum_{t} \left(P(t) - f_P\left((t - t_0) \bmod 24, \vartheta_{ex}, \beta\right) \right)^2$$

$$f_P(0, \vartheta_{ex}, \beta) = f_P(24, \vartheta_{ex}, \beta)$$

$$0 < t_m^{EGH1} < t_m^{EGH1} < 24 \quad (8)$$

$$0 < H^{EGH1}$$

$$0 < H^{EGH2}$$

where

β	is vector of EGH1 and EGH2 functions parameters.

The Particle swarm algorithm [10] was chosen as the numeric optimization algorithm suitable for problem without explicit knowledge of the gradient of function to be optimized. We use MaxDistQuick as a stopping criterion as described in [11]. The optimization is stopped if the maximum distance of the major part of particles is below a threshold *eps* (Fig. 10) or the maximum number of iteration is reached. Fig. 11 depicted serial version of PSO and Fig. 12 parallel version of PSO.

We use these PSO variant:

$$v'_{i,j} = \omega v_{i,j} + c_1 r_1 \left(global\ best_j - x_{i,j}\right) + c_2 r_2 \left(local\ best_{i,j} - x_{i,j}\right) \quad (9)$$

$$x'_{i,j} = x_{i,j} + v'_{i,j} \quad (10)$$

where

n	is the number of particles, i = 1,…,n,
m	is the dimension, j = 1, …, m,
$x_{i,j}$	is the particle position,
$x'_{i,j}$	is the updated particle position,
$v_{i,j}$	is the particle velocity,
ω	is the inertia component,
c_1	is the social component,
c_2	is the cognitive component,
r_1, r_2, r_3	are uniform random numbers ⟨0,1⟩,

$global\ best_j$ is the best global position,
$local\ best_{i,j}$ is the best local particle position.

The number of particles n we usually set two times more than dimension m. Inertia component ω is set about 0.8, social component c_1 is set about 1.4 and cognitive component c_2 is set about 0.6.

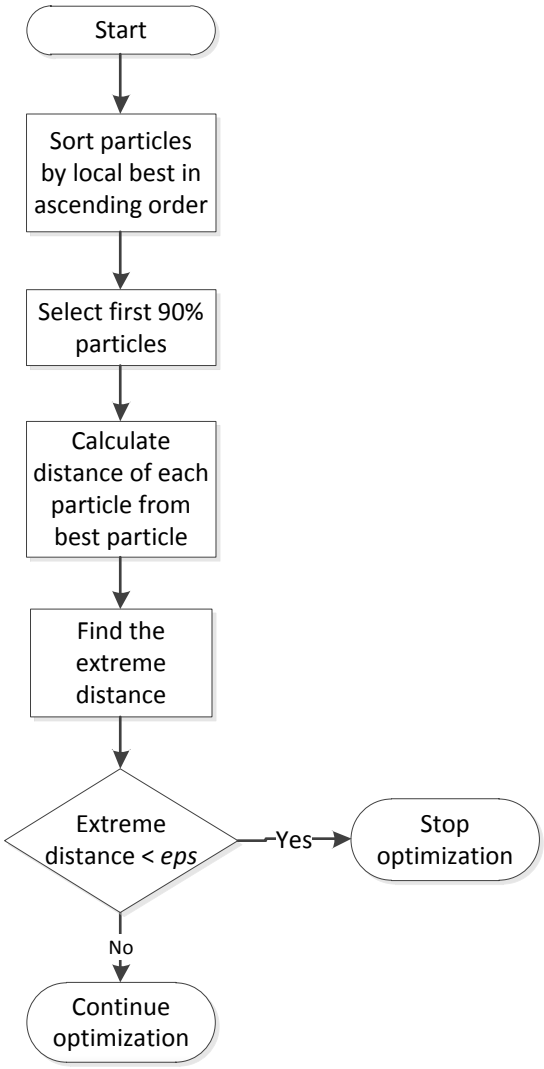

Fig. 10: MaxQuickDist Stopping Criterion

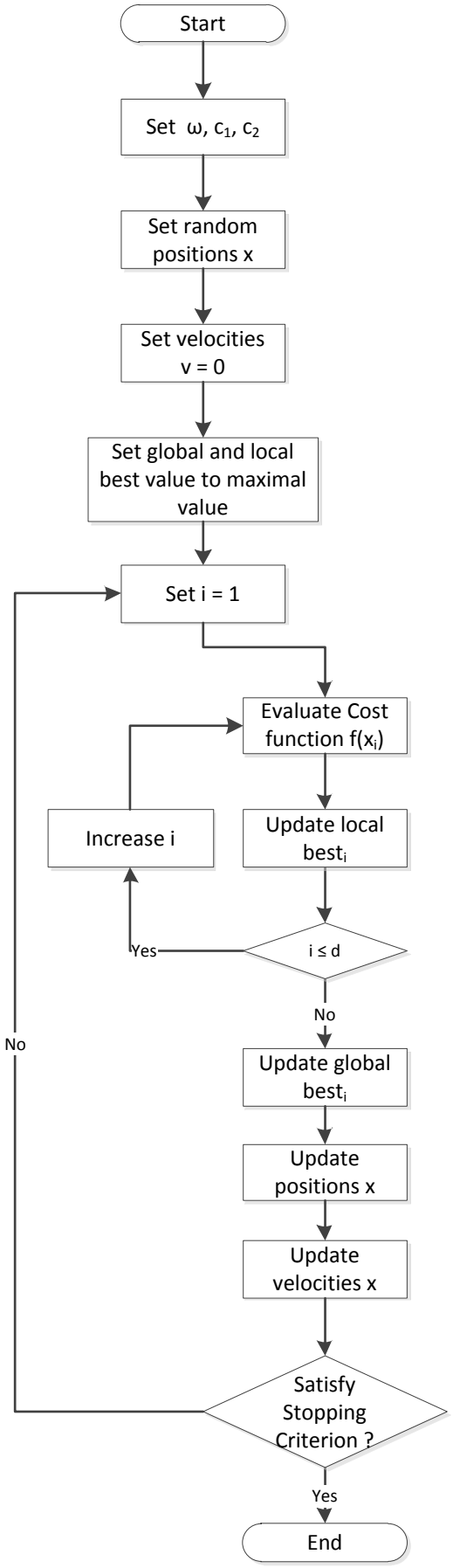

Fig. 11: PSO Serial

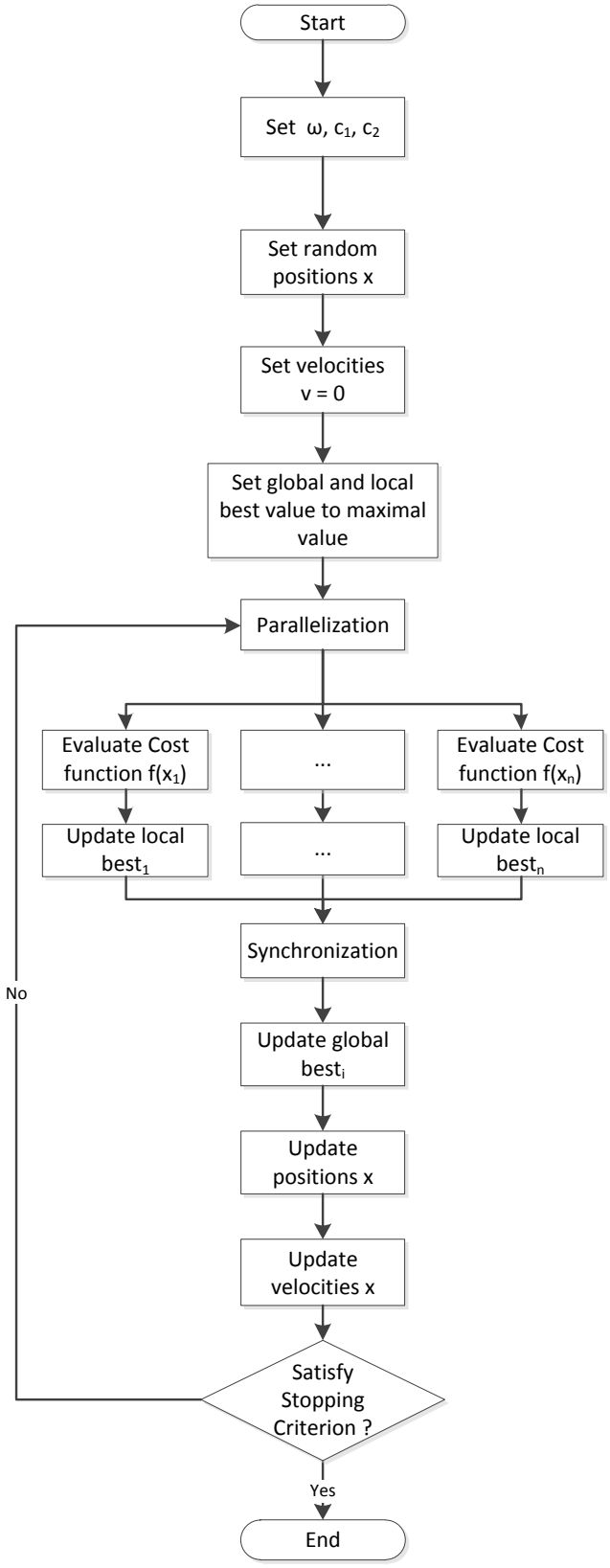

Fig. 12: PSO Parallel

D. Parameters Estimation and Prediction

Parameters are estimated with use of PSO algorithm as depicted in Fig. 13: Parameters estimation and heat load is predicted as depicted in Fig. 14.

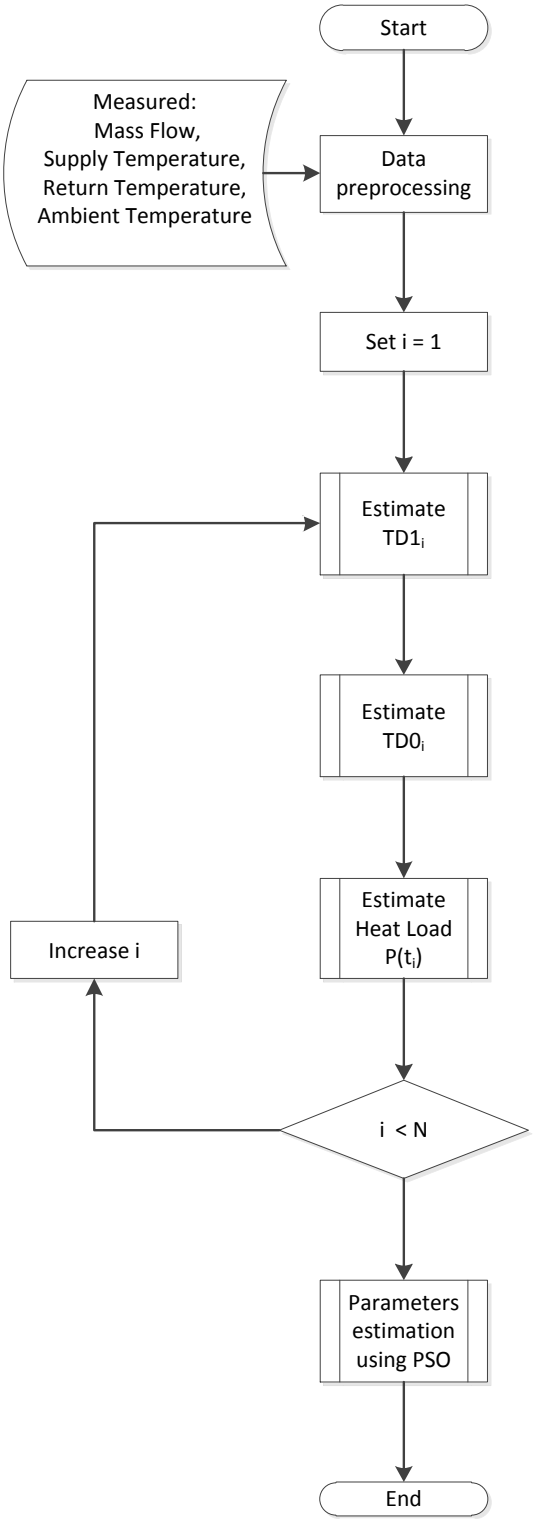

Fig. 13: Parameters estimation

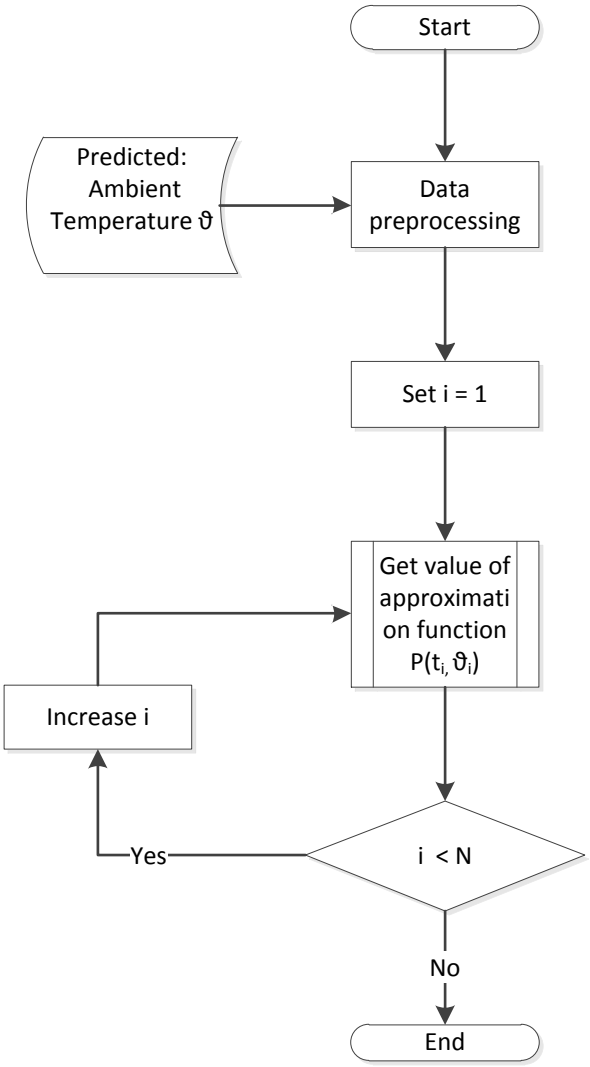

Fig. 14: Heat load prediction

IV. RESULTS

Method was evaluated on data from two CHP plant in Czech Republic. Due to the legal restriction, the names and exact data of CPH cannot be published. Fig. 16 shows comparison of measured and approximated Heat Load at CPH A

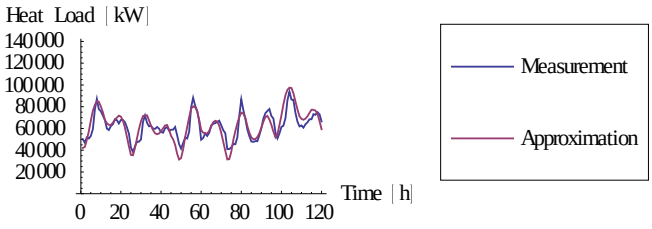

Fig. 15: Heat load approximation (CPH A)

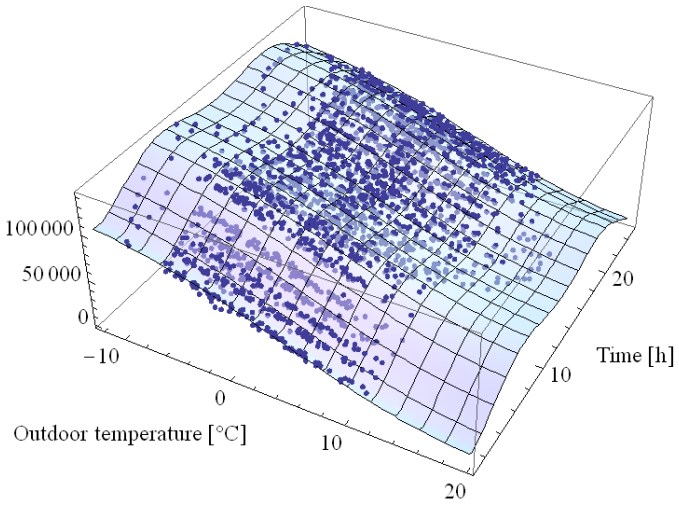

Fig. 16: Comparison of measured and approximated Heat Load (CPH A)

Table 1 shows approximation results as Root Mean Square Error (RMSE), Percentage Average Relative Error (PARE) and Percentage Normalized Root Mean Square Error (PNRMSE) according to:

$$\boldsymbol{RMSE} = \sqrt{\frac{\mathbf{1}}{\boldsymbol{N}}\sum_{\boldsymbol{i=1}}^{\boldsymbol{N}}(\boldsymbol{y_i} - \boldsymbol{\hat{y}_i})^{\mathbf{2}}} \tag{11}$$

$$\boldsymbol{PARE} = \mathbf{100}\sqrt{\frac{\mathbf{1}}{\boldsymbol{N}}\sum_{\boldsymbol{i=1}}^{\boldsymbol{N}}\frac{|\boldsymbol{y_i} - \boldsymbol{\hat{y}_i}|}{|\boldsymbol{y_i}|}} \tag{12}$$

$$\boldsymbol{PNRME} = \mathbf{100}\frac{\boldsymbol{RMSE}}{\boldsymbol{y_{max}} - \boldsymbol{y_{min}}} \tag{13}$$

Table 1: Approximation results

	CHP A	CHP B
	3 month, winter season	3 month, winter season
RMSE [KW]	7395.8	3200.5
PARE [%]	7.34	10.18
PNRMSE [%]	5.99	6.98

V. CONCLUSION

The new method was evaluated on the data of two combined heat and power plant. The results prove the suitability of this method. Next research will be the classification of daily patterns by means of EGH parameters.

ACKNOWLEDGMENT

The work was performed with financial support of research project NPVII-2C06007, by the Ministry of Education of the Czech Republic. The work was also supported by the European Regional Development Fund under the Project CEBIA-Tech No. CZ.1.05/2.1.00/03.0089.

.

REFERENCES

[1] CHRAMCOV, Bronislav. Heat Demand Forecasting for Concrete District HeatingSystem. International Journal of Mathematical Models and Methods in Applied Sciences [online]. 2010, Volume 4, Issue 4, [cit. 2010-11-30]. ISSN 1998-0140.

[2] CHRAMCOV, Bronislav. Forecast of Heat Demand According the Box-Jenkins Methodology for Specific Locality. In Proceedings of 14th WSEAS International Conference on Systems : Latest Trends on Systems. Corfu Island: WSEAS Press, 2010. s. 252-256. ISBN 978-960-474-199-1, ISSN 1792-4235.

[3] CHRAMCOV, Bronislav. Evaluation of Heat Demand Forecast for Specific Localities. In Annals of DAAAM for 2010 & Proceedings of the 21st International DAAAM Symposium. Vienna : DAAM International, 2010. s. 0267-0268. ISBN 978-0-9553018-8-9, ISSN 1726-9779.

[4] Vasek, L., Dolinay, V. Simulation model of heat distribution and consumption in municipal heating network (2010) International Journal of Mathematical Models and Methods in Applied Sciences, 4 (4), pp. 240-248.

[5] Helge L., Benny B., Michael W. A comparison of aggregated models for simulation and operational optimisation of district heating networks, *Energy Conversion and Management*, Volume 45, Issues 7-8, May 2004, pp. 1119-1139, ISSN 0196-8904

[6] Vařacha, P. Impact of Weather Inputs on Heating Plant - Agglomeration Modeling. *Proceedings of the 10th WSEAS International Conference on Neural Networks*, Prague 2009, Mastorakis, N., pp. 159-162, ISBN 978-960-474-065-9

[7] Heller J. Heat-load modelling for large systems, Applied Energy, Volume 72, Issue 1, May 2002, Pages 371-387, ISSN 0306-261

[8] Saarinen, Linn. Modelling and control of a district heating system. Uppsala, 2008. 67 s. Uppsala University. ISSN 1650-8300.

[9] Jianwei Li, Comparison of the capability of peak functions in describing real chromatographic peaks, *Journal of Chromatography A*, Volume 952, Issues 1-2, 5 April 2002, Pages 63-70, ISSN 0021-9673, DOI: 10.1016/S0021-9673(02)00090-0.

[10] Kennedy J., Eberhart R. Particle Swarm Optimization. *Proceedings of IEEE International Conference on Neural Networks*. IV. pp. 1942-1948.

[11] Martí L., García J., Berlanga, A., Molina, M. An approach to stopping criteria for multi-objective optimization evolutionary algorithms: the MGBM criterion. *In Proceedings of the Eleventh Conference on Congress on Evolutionary Computation.* Trondheim, Norway, May 18 - 21, 2009. IEEE Press, Piscataway, NJ, 1263-1270.